

Optimized Configuration of Hybrid Electric-Hydrogen Energy Storage System Considering Carbon Trading and Wind Power Fluctuation Smoothing

Pengyu Wei¹, Dongsheng Cai^{1*}, Chiagoziem Chima Ukwuoma¹, Olisola Bamisile¹, Qi Huang^{1,2}

1 College of Nuclear Technology and Automation Engineering, Chengdu University of Technology, Sichuan P.R., 610059, China

2 School of Information Engineering, Southwest University of Science and Technology, Maiyang, Sichuan P.R., China

(*Corresponding Author: caidongsheng@cdut.edu.cn)

ABSTRACT

Low-carbon mode is an important way to face global warming and extreme climate problems, and countries around the world have invested huge amounts of money in exploring perfect low-carbon energy-saving systems, and hydrogen energy, as the cleanest energy source, has been applied in this process. This paper proposes an optimal configuration model of electric-hydrogen hybrid energy storage system considering carbon trading and wind power fluctuation smoothing. Firstly, the basic principle of carbon trading is expressed, and on the basis of which a carbon trading stepwise cost model is proposed; then, the initial wind power signal is decomposed into the power generation demand portion and the hydrogen production portion; on the carbon trading cost model and the decomposition of the wind power signal, the hybrid electric-hydrogen system is constructed. On the basis of the carbon trading cost model and wind power signal decomposition, the hybrid electric-hydrogen system is constructed, and the optimization strategy is proposed under the objectives of maximizing wind energy consumption and optimizing the economy of hydrogen energy utilization. The study shows that under the stepped carbon trading model, the maximum utilization of clean energy can be obtained by smoothing the fluctuation of wind power, and the hydrogen produced can be sold to obtain economic benefits for reducing the cost of hydrogen production equipment.

Keywords: carbon trading, wind power volatility smoothing, hydrogen production, hybrid energy storage

1. INTRODUCTION

Facing the energy crisis and greenhouse gas emissions, more and more countries and regions are

applying natural gas as an alternative to other energy sources with higher carbon emissions. Hydrogen, as a clean energy source, burns theoretically with almost no carbon emissions, and thus the hydrogen doping ratio of natural gas and hydrogen blends is increasingly being studied.

In terms of hydrogen mixed combustion, hydrogen is mainly involved in natural gas combustion, as well as a small amount of research in ammonia with n-pentane. Literature [1] investigated the ammonia on its combustion stability and misfire problems, and showed that the proper ammonia-hydrogen mixing ratio is critical stability. Literature [2] studied delay time of n-pentane and found that hydrogen addition had a weak ignition promotion effect.

In the study of blending with natural gas, literature [3], investigated the hydrogen blending ratio on combustion rate and maximum overpressure and found that increased hydrogen content significantly improves the combustion efficiency, and the maximum overpressure increases rapidly when the ratio exceeds 40%. Literature [4], analyzed its feasibility and economics. Literature [5] applied energy to an internal combustion engine and investigated the emission performance and combustion characteristics for different hydrogen percentage ratios.

In addition to this, there is an analysis and investigation of its safety, literature [6] for hydrogen doped natural gas leakage diffusion characteristics were investigated. Literature [7] showed that increasing the proportion of hydrogen increases the peak temperature. In addition to this there are emission characterization studies, literature [8] focuses on the advantages of low carbon dioxide production with low NO_x emissions during low-oxygen dilution of mixed hydrogen methane, assessing the formation and reduction of NO_x in the light

combustion of methane/hydrogen co-fired fuels with no hydrogen to a pure hydrogen mixing ratio.

New energy sources are involved in the system to generate more environmentally friendly possibilities, regarding wind power fluctuation smoothing, literature [9] considers the grid AC current and gas hydraulics in the gas pipeline network to calculate the coordinated operation strategy, which can effectively smoothen the power fluctuations in the distribution network. Literature [10] adopts the method of dual source voltage coordinated control to solve the load power. Literature [11], analyzed real condition control, and improved the strategy to make solar-electric power efficiency fluctuations reduced. Literature [12], proposed an energy scheduling strategy using dual fuzzy logic algorithms to take advantage of thermal storage, and the results showed that air source heat pump energy is effective for PV fluctuation stabilization. In literature [13] proposed to solve the power fluctuation of doubly-fed induction generator to achieve load voltage stabilization under various transient perturbations as well as power regulation under wind speed variations.

However, for the study of carbon emissions trading, the literature [14] centralized optimization of power system impacts using carbon price can achieve satisfactory convergence accuracy and less computation time. Literature [15], proposed a demand-side two-tier carbon trading scheme, where the upper tier constructs a customized model based on the step-optimal carbon price, and the lower tier proposes a carbon trading mechanism based on a competitive auction scheme. The feasibility of demand-side two-tier carbon trading is demonstrated. Literature [16], explored the carbon footprint of the Belt and Road, improving carbon efficiency is the most important driver, and the carbon footprint has gradually shifted from China India to Southeast Asia, West Asia and Africa. Literature [17], analyzed the carbon emissions trading mechanism in China. The study suggests that the future national carbon market should take full account of imbalances between groups.

Therefore, this paper proposes a model for hybrid hydrogen energy and levelized wind power to address the above issues.

2. METHOD AND FORMULATION

2.1 Hydrogen-doped energy system

The system consists of hydrogen doped gas turbine(HDGT), gas boiler(GB), wind turbine(WT), electrical storage unit(ESU), thermal storage unit(TSU),

and electrically heated boiler(EHB). The load consists of electrical and thermal loads, the electrical loads are supplied by the WT, ESU, and the thermal loads are supplied by the GB, TSU, and EHB.

Energy storage and P2G, as flexible resources, can flexibly match the change of renewable energy output by utilizing their energy time-shift characteristics, and can coordinate through the energy management system to obtain the optimal profit while satisfying the load demand and safety.

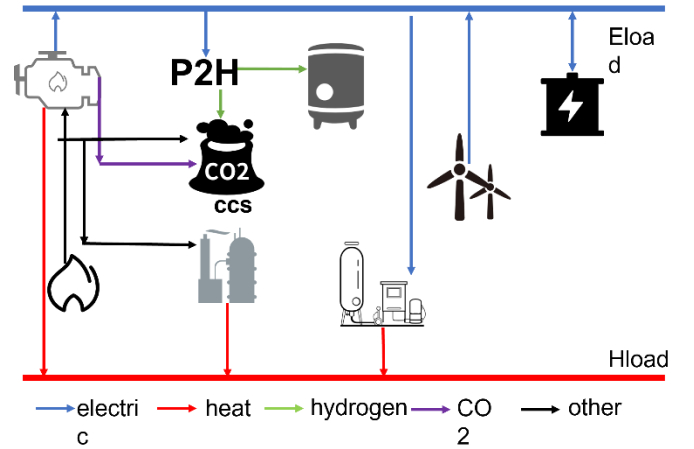


Fig. 1 System Structure Drawing

2.2 Methods

Hydrogen doped gas turbine, the gas turbine is hydrogen doped with natural gas in the range of 10%-20% content, the mathematical model of the gas turbine is as follows:

$$\begin{cases} P_{chp}^t = (Q_{CH_4, chp}^t + Q_{H_2, chp}^t) \eta_{chp}^P \\ H_{chp}^t = (Q_{CH_4, chp}^t + Q_{H_2, chp}^t) \eta_{chp}^H \\ Y_{H_2, chp}^t = \frac{Q_{H_2, chp}^t / L_{H_2}}{Q_{CH_4, chp}^t / L_{CH_4} + Q_{H_2, chp}^t / L_{H_2}} \end{cases}$$

where, η_{chp}^P , η_{chp}^H are the electrical and heat efficiency of GT; $Q_{CH_4, chp}^t$, $Q_{H_2, chp}^t$ are the volume relative parameter of CH4 and H2; L_{CH_4} , L_{H_2} are theoretical molar volume of CH4 and H2; $Y_{H_2, chp}^t$ is the hydrogen doping rate.

Hydrogen-doped gas boilers, the relevant standards require gas boilers to use hydrogen-doped mixed gas, hydrogen molar mass ratio to remain in the range of 2%-20%, gas boiler mathematical modeling is as follows:

$$\begin{cases} H_{GB}^t = (Q_{CH_4,GB}^t + Q_{H_2,GB}^t)\eta_{GB} \\ Y_{H_2,GB}^t = \frac{Q_{CH_4,GB}^t \rho_{CH_4} / M_{H_2} L_{H_2}}{Q_{CH_4,GB}^t \rho_{CH_4} / M_{CH_4} L_{CH_4} + Q_{H_2,GB}^t \rho_{H_2} / M_{H_2} L_{H_2}} \end{cases}$$

where, η_{GB} is heat efficiency of GB, $Q_{CH_4,GB}^t$, $Q_{H_2,GB}^t$ are the volume relative parameter of CH4 and H2; ρ_{CH_4} , ρ_{H_2} are density of CH4 and H2; L_{CH_4} , L_{H_2} are bulk of them; M_{CH_4} , M_{H_2} are the molar mass of them; $Y_{H_2,GB}^t$ is the hydrogen doping rate.

Hydrogen storage operating power limitations are as follows:

$$\begin{cases} P_{EL}^{stab\ min} \leq P_{EL,n}^{stab} \leq 1.2P_{EL}^{stab\ rated} \\ P_{FC}^{stab\ min} \leq P_{FC,n}^{stab} \leq P_{FC}^{stab\ rated} \\ P_{EL,n}^{stab} P_{FC,n}^{stab} \leq 0 \end{cases}$$

where, $P_{EL}^{stab\ min}$ is the minimum power limit of the electrolyzer; $P_{FC}^{stab\ min}$ is the minimum power limit of the fuel cell.

The hydrogen storage constraints include the following constraints in addition to the conversion characteristic constraints of the electrolyzer and the fuel cell:

$$v_{STO,t}^{stabin} = v_{EL,t}^{stab}$$

$$v_{STO,t}^{stabout} = v_{FC,t}^{stab}$$

$$SOH_n^{stab} - SOH_{n-1}^{stab} = \left(\frac{v_{STO,n}^{stabin}}{m_{STO}^{stab\ rated}} - \frac{v_{STO,n}^{stabout}}{m_{STO}^{stab\ rated}} \right) \Delta t$$

$$SOH_{min}^{stab} \leq SOH_n^{stab} \leq SOH_{max}^{stab}$$

where, $v_{STO,n}^{stabin}$, $v_{STO,n}^{stabout}$ are the gas volume in and out tank; SOH_{min}^{stab} , SOH_{max}^{stab} are the work depth of hydrogen tank; $v_{EL,t}^{stab}$, $v_{FC,t}^{stab}$ are the electrolysis rate and fuel cell rate.

The electrochemical energy storage with charge operating state constraints is as follows:

$$SOC_n - SOC_{n-1} = \left(\frac{P_{BAT,n}^{ch}}{E_{BAT}^{rated}} \eta_{BAT} - \frac{P_{BAT,n}^{disch}}{E_{BAT}^{rated}} \eta_{BAT} \right) \Delta t$$

$$SOC_{min} \leq SOC_n \leq SOC_{max}$$

where, SOC_{min} , SOC_{max} are the min and max charge and discharge; $P_{BAT,n}^{ch}$, $P_{BAT,n}^{disch}$ are charge and discharge power; η_{BAT} is heat efficiency.

The thermal and electrical storage models that also consider their own power consumption are as follows:

$$\begin{cases} S_{HS}^t = S_{HS}^{t-1} (1 - \delta_{HS}) + (H_{HS}^{t,ch} \eta_{HS}^{ch} - H_{HS}^{t,dis} / \eta_{HS}^{dis}) \Delta t \\ S_{ES}^t = S_{ES}^{t-1} (1 - \delta_{ES}) + (P_{ES}^{t,ch} \eta_{ES}^{ch} - P_{ES}^{t,dis} / \eta_{ES}^{dis}) \Delta t \end{cases}$$

where, η_{HS}^{ch} , η_{HS}^{dis} are the electrical energy charging and discharging efficiency; S_{HS}^t , S_{ES}^t are the state of hydrogen storage and electric storage.

Electric heating boiler is as follows:

$$H_{EB}^t = \eta_{EB} P_{EB}^t$$

Where, H_{EB}^t is the real heat production power; P_{EB}^t is heat production power.

2.3 Theory

The reconstruction of IMF is to superimpose the components bands according to the given index to obtain the components. The reconstruction method is divided into high-frequency reconstruction and low-frequency reconstruction components of each order according to the EMD decomposition results superimposed from top to bottom, and the reconstruction formula is as follows:

$$\begin{cases} f2c(1) = IMF1 \\ f2c(2) = IMF1 + IMF2 \\ \vdots \\ f2c(p+1) = IMF1 + IMF2 + \dots + IMFp + res \end{cases}$$

The low-frequency reconstruction generates the low-frequency reconstruction components of each order according to the bottom-up superposition of the EMD decomposition results, which is reconstructed as following.

$$\begin{cases} c2f(1) = res \\ c2f(2) = res + IMFp \\ \vdots \\ c2f(p+1) = res + IMFp + \dots + IMF1 \end{cases}$$

Calculation of emission allowances as following.

$$\begin{cases} P_{CCS}^t = e_c E_2^t \\ P_{CCS,sum}^t = P_{CCS}^t + P_B \end{cases}$$

Where, e_c is consumption of CO2, $e_c = 0.269 \text{ MW-h/t}$; E_2^t is the mass of CO2 processed by the regeneration tower at the moment t , and its value is determined by the system optimization scheduling.

Because of the great energy consumption, this paper adopts the CCS with flue gas shunt, and achieves the purpose by actively discharging CO2, the specific expressions are as follows.

$$E_1^t = E^t - e_1^t$$

where: E_1^t is the total emissions at t moment and the amount of CO₂ absorbed by the CCS; e_1^t is for the amount of CO₂ discharged into the atmosphere by the flue gas shunt at t moment.

Since consumption is mainly concentrated in the regeneration tower, in this paper, a liquid storage device is added to the CCS to carry out the energy time shift and effectively decouple the CO₂, absorption and regeneration processes. The liquid storage equipment contains lean and rich liquid storage equipment, and represent the storage capacity of rich and lean liquid storage equipment, respectively, and the expression is shown as follows.

$$\begin{cases} V_F^t = V_F^{t-1} + v_{F,in}^t - v_{F,out}^t \\ V_P^t = V_P^{t-1} + v_{P,in}^t - v_{P,out}^t \end{cases}$$

where, V_F^t is the volume flow rate into and out of the lean liquid storage device at moment t ; V_P^t is the volume flow rate into and out of the rich liquid storage at moment t .

The gratuitous allocation adopted in most of the literature is used. In this paper, the carbon emission right allocation approach is used, and the objects with carbon emission right allocation include gas turbines and coal-fired units.

$$E_{quota}^t = \lambda_p^{chp} P_{chp}^t + \lambda_H^{chp} H_{chp}^t + \lambda_p^{th} P_{th}^t$$

Calculation of actual carbon emissions(ACE)

The ACE refers to the net emission of CO₂ produced by the system minus the amount of CO₂ sequestered and processed by P2G. The net CO₂ emission of the system consists of two parts, e_1^t and e_2^t , which are the CO₂ that is directly emitted into the atmosphere through the flue gas diversion and the CO₂ that is indirectly emitted into the atmosphere due to the inability of carbon capture efficiency to reach 100%, and is calculated by the Eq.

$$\begin{cases} e_{air}^t = e_1^t + e_2^t \\ e_2^t = (1 - \eta_c) E_1^t \end{cases}$$

where the total amount of CO₂ produced by the system, E , is calculated as follows.

$$E^t = \varepsilon_1 (Q_{CH_4,GB}^t + Q_{CH_4,chp}^t) + \varepsilon_2 P_{th}^t$$

where, P_{th}^t is capacity of TSU; E^t is the carbon emissions corresponding to the consumption of natural gas per unit power.

To more strictly restrain carbon emissions, this paper is analogous to the ladder tariff, in emissions

interval calculation of carbon trading costs, when quota more than a given interval, the excess portion of the increase price; when the emissions are lower than the carbon quota, will be more than the right to sell carbon emissions to obtain revenues, and the introduction of compensation coefficients to increase the reduction of emissions. The calculation model is as follows:

$$f_{co_2}^t = \begin{cases} -\chi(2+3\delta)L + \chi(1+3\delta)(e_{jy}^t + 2L), & e_{jy}^t \leq -2L \\ -\chi(1+\delta)L + \chi(1+2\delta)(e_{jy}^t + L), & -2L < e_{jy}^t < -L \\ \chi(1+\delta)e_{jy}^t, & -L < e_{jy}^t \leq 0 \\ \chi e_{jy}^t, & 0 < e_{jy}^t \leq L \\ \chi L + \chi(1+\theta)(e_{jy}^t - L), & L < e_{jy}^t < 2L \\ \chi(2+\theta)L + \chi(1+2\theta)(e_{jy}^t - 2L), & 2L \leq e_{jy}^t \end{cases}$$

where, $f_{co_2}^t$ is the carbon trading base price; L is the length of the carbon emission interval; e_{jy}^t is the growth rate of the carbon trading price; δ is the compensation coefficient, θ is the cost of carbon trading at the moment t .

$$\min F = F_{co_2} + F_f + F_{th1} + F_{th2} + F_{buy} + F_{cur}$$

where F is the total cost, which contains six components, namely F_{co_2} carbon trading cost, F_f carbon sequestration cost, F_{th1} start-up and shutdown cost of coal power units, F_{th2} coal consumption cost, F_{buy} , purchased gas cost, and F_{cur} abandoned wind cost.

Carbon trading and carbon sequestration costs:

$$F_{CO_2} = \sum_{t=1}^T f_{co_2}^t$$

$$F_f = \sum_{t=1}^T (c_f E_{2,storage}^t)$$

where, $f_{co_2}^t$ is cost of sequestering unit mass CO₂.

Coal-fired unit startup and shutdown and coal consumption costs.

$$F_{th1} = S \sum_{t=2}^T (u_{th}^t (1 - u_{th}^{t-1}) + u_{th}^{t-1} (1 - u_{th}^t))$$

$$F_{th2} = \sum_{t=1}^T (a_{th} (P_{th}^t)^2 + b_{th} P_{th}^t + c_{th})$$

where, S is the startup and shutdown cost; u_{th}^t is a 0-1 variable, indicating the state; a_{th} , b_{th} , c_{th} are the coal consumption.

Wind abandonment costs

$$F_{cur} = \sum_{t=1}^T (c_{cur} P_{cur}^t)$$

where, c_{cur} is the penalty cost of abandoned wind.

Gas purchase cost.

$$F_{buy} = \sum_{t=1}^T (c_{buy} Q_{buy}^t)$$

where, Q_{buy}^t is the power corresponding to the natural gas purchased by the system at time t .

3. RESULTS

The system constructed is a system containing electric and thermal loads, in which wind energy is accessed to provide energy supply through EMD decomposition technology, the data source is an industrial park in Shandong Province, China, and the relevant thermal load and electric load in the park are shown in Fig. 2, which shows that the load in the park conforms to the conventional load characteristics, and the thermal demand is greater from 0:00 to 10:00, and the electric demand from 10:00 to 24:00 is greater. The solution is obtained by using Cplex commercial solver.

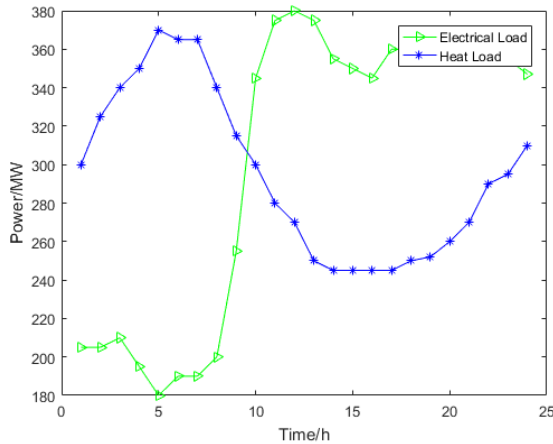


Fig. 2. Electrical and thermal loads

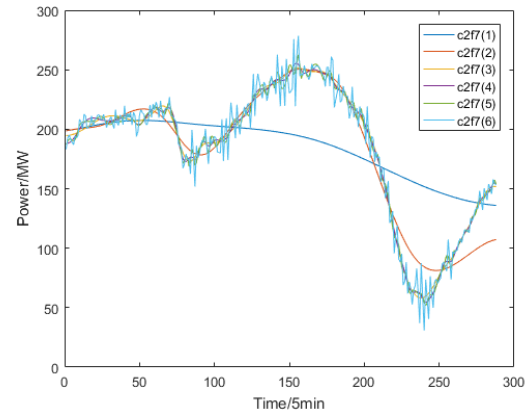


Fig. 3. Low-order reconstructed components of wind power data

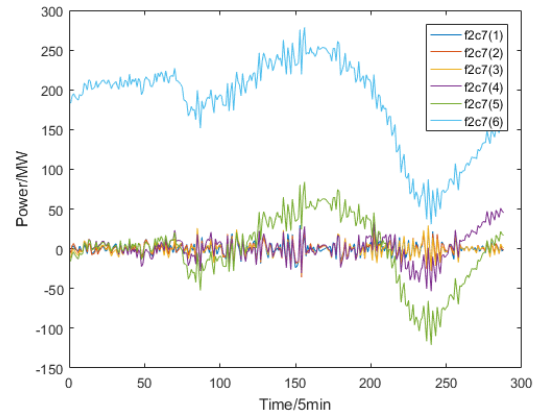


Fig. 4. Higher-order reconstructed components of wind power data

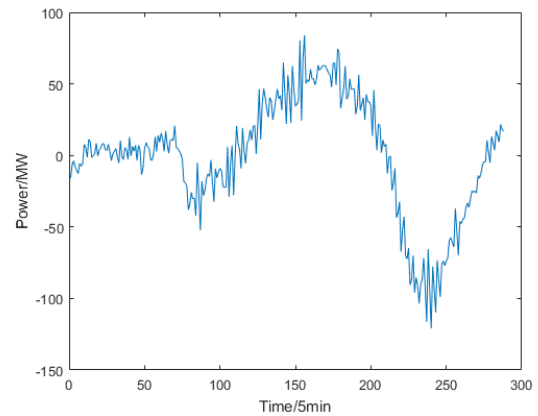


Fig. 5. Storage leveling power

The results of wind power fluctuation smoothing are as follows, Fig. 3 shows the low-order data, Fig. 4 shows the high-order data, and Fig. 5 shows the energy storage smoothing power. Higher order components are obtained for power participation and for lower order components, wind abandonment is selected. The higher order components are averaged by summing to get the turbine output per unit hour for subsequent participation in energy balancing.

For the carbon trading characteristics of the system, and Fig. 6 shows the carbon quota and actual carbon trading. From the figure, it can be seen that the carbon quota is not enough to meet the user's carbon emission demand in most of the time of the day (10:00-24:00), so carbon trading is needed for regulation. The power of carbon trading is shown in the figure, which is homologous to the volatility of the actual carbon emission curve, i.e., the more carbon is emitted, the more carbon is traded, but the traded carbon cannot exceed the carbon quota limited by the government.

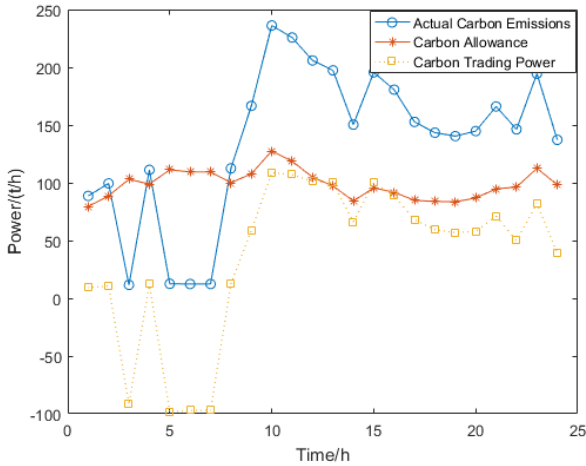


Fig. 6. Carbon allowances versus actual carbon trading and carbon emission curves

The results of the internal operation characteristics of CCS are shown in Fig. 7, the initial state, the rich and poor liquids contain equal amounts, at 4:00-8:00 the rich liquid absorbs more CO₂, the carbon content gradually rises, and at this time it is also in the moment of higher carbon emissions, due to the heating load of the night carbon emissions are larger. After that, with the reduction of heating load, carbon emission decreases, and the poor liquid starts to draw carbon from the rich liquid, and finally reaches the steady state equilibrium. This operating state shows that the process of carbon trading is closely related to the load usage, especially for the heat load using gas boilers, which produce higher carbon emissions.

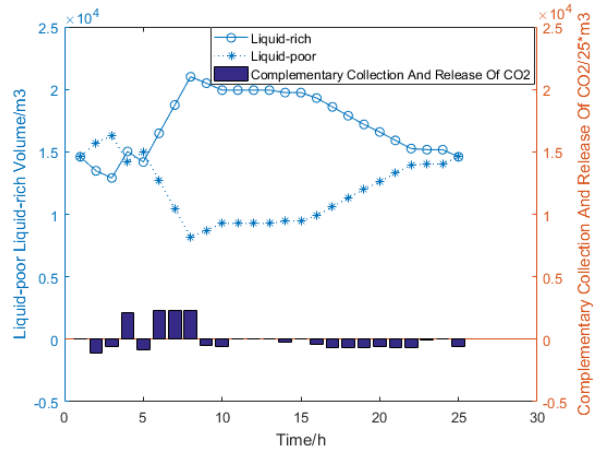


Fig. 7. CO₂ trading curves for rich and poor liquids

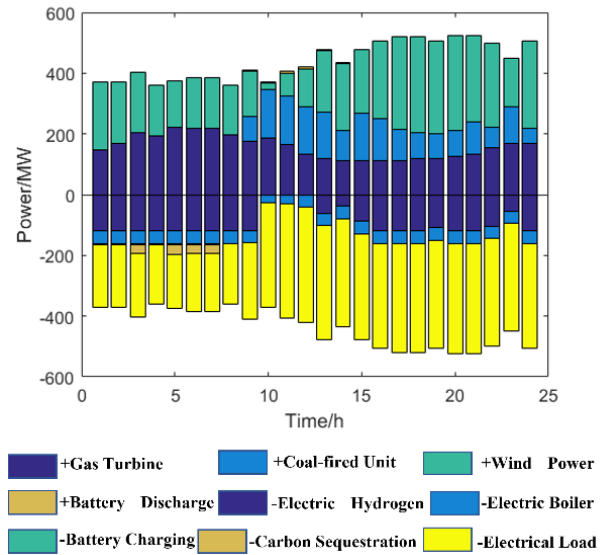


Fig. 8. Operating conditions of the components of the system's electrical balance

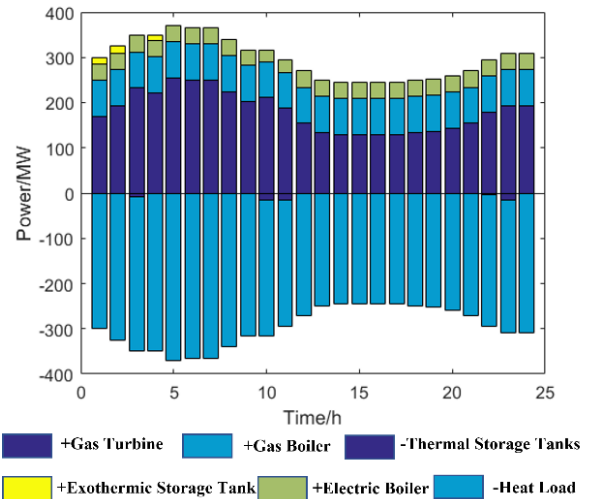


Fig. 9. Operating conditions of the components of the system heat balance

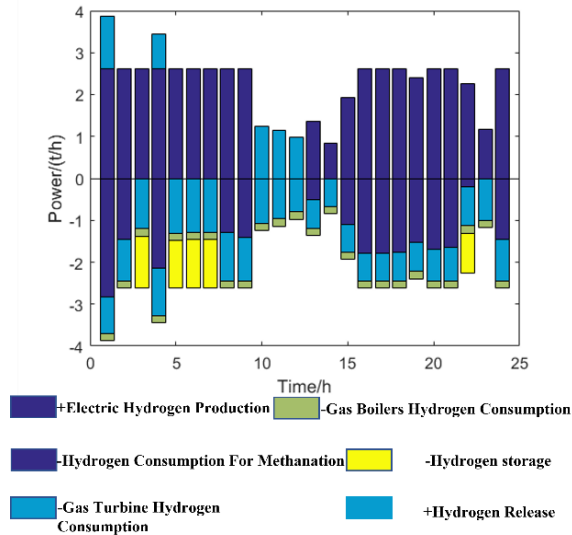


Fig. 10. Operating conditions of the components of the system hydrogen balance

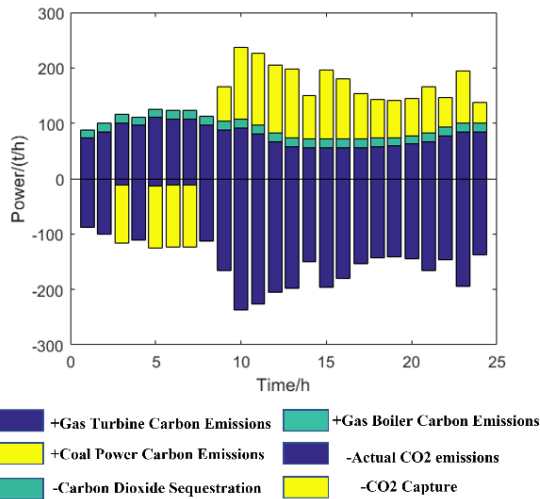


Fig. 11. System CO2 emission balance and operating conditions of each component

4. DISCUSSION

For the overall operating conditions of the system, the results shown in Figs. 8,9,10,11 below are obtained for the system electric energy balance, system thermal energy balance, system hydrogen energy balance and system carbon emission balance.

For the electric energy balance, it can be seen through the operating conditions that the power supply measurement is mainly provided by gas turbines, thermal power units, wind turbines, and due to the addition of wind energy, the participation of thermal power units in the electric balance can be effectively reduced, such as 0:00-8:00 high-pollution thermal power generating units are supplied completely by the wind power generation. For the electricity side, excess electricity is used for electric hydrogen production, while

the others are mainly basic electricity loads. Particularly noteworthy is the operation of the carbon capture unit from 3:00-7:00, which consumes some electrical energy.

For the thermal energy balance, the main contributions are the steam and gas turbines, which generate a lot of thermal energy. Thermal storage devices are less utilized due to poor characteristics in terms of thermal energy storage, which is determined by their specific energy endowment; thermal energy is not as convenient to transmit as electrical energy, which is best consumed locally, and the problem of retention after storage is difficult to overcome.

For the balance of characteristics of CO₂, the main emissions are from GB, and the operation of carbon capture devices reduces carbon emissions. However, in terms of cost, it will increase cost of electricity and equipment, so CCS needs to be considered in a balanced way.

The results of the study on the amount of hydrogen doping are shown in the following table.

Table. 1. Hydrogen doping with total cost and CO₂ emissions

hydrogen doping	Total cost/million RMB	CO ₂ emissions/t
2%	498.75	2871.8
6%	498.37	2880.6
10%	497.88	2887.6
14%	497.27	2899.5
18%	496.60	2907.3

5. CONCLUSIONS

In this paper, by establishing an electric-hydrogen storage system, and considering wind power leveling. It obtains the internal operating conditions of the carbon capture device, as well as the overall electric, thermal, and hydrogen energy utilization conditions of the system and the collaborative operating states of the components in carbon emissions, and study the impact of hydrogen participation in the gas turbine on the system objectives. The study shows that within the safe operation range, hydrogen doping will improve the system energy utilization, and the larger the proportion, the smaller the operation cost, but also the larger the carbon emission.

ACKNOWLEDGEMENT

The authors gratefully acknowledge the support by the National Natural Science Foundation of China (NFSC, Grant No. 52007025).

DECLARATION OF INTEREST STATEMENT

The authors declare that they have no known competing financial interests or personal relationships that could have appeared to influence the work reported in this paper. All authors read and approved the final manuscript.

REFERENCE

[1]J. Li, R. Zhang, J. Pan, H. Wei, G. Shu, and L. Chen, "Ammonia and hydrogen blending effects on combustion stabilities in optical SI engines," *Energy Convers. Manag.*, vol. 280, p. 116827, Mar. 2023.

[2]X. Jiang, R. Zhang, and F. Deng, "Effects of equivalence ratio and blending ratio on the ignition delays of n-pentane/hydrogen mixtures under engine relevant pressure," *Fuel*, vol. 288, p. 119669, Mar. 2021.

[3]C. Zhou, Z. Yang, G. Chen, Q. Zhang, and Y. Yang, "Study on leakage and explosion consequence for hydrogen blended natural gas in urban distribution networks," *Int. J. Hydrog. Energy*, vol. 47, no. 63, pp. 27096–27115, Jul. 2022.

[4]M. Mayrhofer, M. Koller, P. Seemann, R. Prieler, and C. Hochenauer, "Assessment of natural gas/hydrogen blends as an alternative fuel for industrial heat treatment furnaces," *Int. J. Hydrog. Energy*, vol. 46, no. 41, pp. 21672–21686, Jun. 2021.

[5]X. Zhen, X. Li, Y. Wang, D. Liu, and Z. Tian, "Comparative study on combustion and emission characteristics of methanol/hydrogen, ethanol/hydrogen and methane/hydrogen blends in high compression ratio SI engine," *Fuel*, vol. 267, p. 117193, May 2020.

[6]Y. Su, "Numerical investigation on the leakage and diffusion characteristics of hydrogen-blended natural gas in a domestic kitchen," *Renew. Energy*, 2022.

[7]M. H. Dinesh, J. K. Pandey, and G. N. Kumar, "Study of performance, combustion, and NO_x emission behavior of an SI engine fuelled with ammonia/hydrogen blends at various compression ratio," *Int. J. Hydrog. Energy*, vol. 47, no. 60, pp. 25391–25403, Jul. 2022.

[8]S. Xu, "NO formation and reduction during methane/hydrogen MILD combustion over a wide range of hydrogen-blending ratios in a well-stirred reactor," 2023.

[9]Y. Jiang et al., "Coordinated operation of gas-electricity integrated distribution system with multi-CCHP and distributed renewable energy sources," *Appl. Energy*, vol. 211, pp. 237–248, Feb. 2018.

[10]L. Tan et al., "Coordinated Source Control for Output Power Stabilization and Efficiency Optimization in WPT

Systems," *IEEE Trans. Power Electron.*, vol. 33, no. 4, pp. 3613–3621, Apr. 2018.

[11]H. Yan, D. Chong, Z. Wang, M. Liu, Y. Zhao, and J. Yan, "Dynamic performance enhancement of solar-aided coal-fired power plant by control strategy optimization with solar/coal-to-power conversion characteristics," *Energy*, vol. 244, p. 122564, Apr. 2022.

[12]L. Yang, "Energy regulating and fluctuation stabilizing by air source heat pump and battery energy storage system in microgrid," *Renew. Energy*, 2016.

[13]R. Yang, J. Jin, Q. Zhou, M. Zhang, S. Jiang, and X. Chen, "Superconducting Magnetic Energy Storage Integrated Current-source DC/DC Converter for Voltage Stabilization and Power Regulation in DFIG-based DC Power Systems," *J. Mod. Power Syst. Clean Energy*, vol. 11, no. 4, pp. 1356–1369, 2023.

[14]T. Qian, W. Tang, and Q. Wu, "A fully decentralized dual consensus method for carbon trading power dispatch with wind power," *Energy*, vol. 203, p. 117634, Jul. 2020.

[15]Z. Yan et al., "Bi-Level Carbon Trading Model on Demand Side for Integrated Electricity-Gas System," *IEEE Trans. Smart Grid*, vol. 14, no. 4, pp. 2681–2696, Jul. 2023.

[16]Q. Lu et al., "Imbalance and drivers of carbon emissions embodied in trade along the Belt and Road Initiative," *Appl. Energy*, vol. 280, p. 115934, Dec. 2020.

[17]X. Fan, X. Li, J. Yin, L. Tian, and J. Liang, "Similarity and heterogeneity of price dynamics across China's regional carbon markets: A visibility graph network approach," *Appl. Energy*, vol. 235, pp. 739–746, Feb. 2019.